Journal of Low Temperature Physics
https://doi.org/10.1007/s10909-022-02921-7

Sensitivity Modeling for LiteBIRD

T. Hasebe[1] · P. A. R. Ade[2] · A. Adler[3] · E. Allys[4] · D. Alonso[5] · K. Arnold[6], et al. *[full author details at the end of the article]*

Received: 1 November 2021 / Accepted: 1 November 2022

Abstract

LiteBIRD is a future satellite mission designed to observe the polarization of the cosmic microwave background radiation in order to probe the inflationary universe. *LiteBIRD* is set to observe the sky using three telescopes with transition-edge sensor bolometers. In this work we estimated the LiteBIRD instrumental sensitivity using its current design. We estimated the detector noise due to the optical loadings using physical optics and ray-tracing simulations. The noise terms associated with thermal carrier and readout noise were modeled in the detector noise calculation. We calculated the observational sensitivities over fifteen bands designed for the LiteBIRD telescopes using assumed observation time efficiency.

Keywords Cosmology · Astronomy · CMB · Satellite · Sensitivity · Detector noise

1 Introduction

LiteBIRD—the Lite (Light) satellite for the study of B mode polarization and Inflation from cosmic background Radiation Detection—is a large class satellite mission proposed by the Institute of Space and Astronautical Science (ISAS), Japan Aerospace Exploration Agency (JAXA), dedicated to the observation of the polarization of the cosmic microwave background (CMB) radiation, with the aim of testing the hypothesis of the inflationary Universe [1]. The targeted sensitivity of *LiteBIRD* is $\delta r \leq 1.0 \times 10^{-3}$, where δr is uncertainty of the tensor-to-scalar ratio, r. This sensitivity enables us to test major single-field inflation models including R^2 inflation [2].

To validate the performance of the instrumental design and to optimize this design, we calculated the sensitivity of the different frequency bands and evaluated the impact on δr [3]. For instance, a design comparison of the HFT using noise calculations is reported in [4].

The sensitivity of the current design of *LiteBIRD* was presented in [1] and [3]. This paper presents the methodology of sensitivity calculations for the current *LiteBIRD* configuration [3], following the BoloCalc method [5], developed to estimate the sensitivities of CMB experiments. The sensitivity calculation for *LiteBIRD* specifically estimates the optical loading by simulating the beam shape of the detector, spillover and the reflection in the optical system.

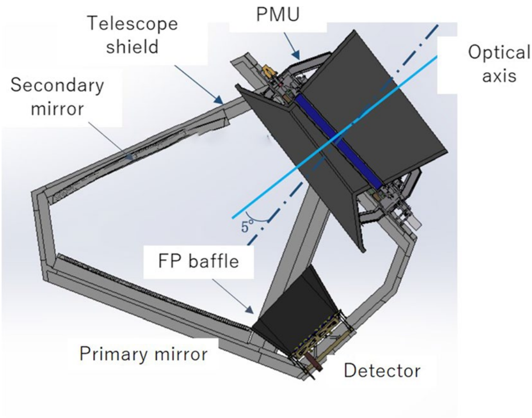

Fig. 1 Schematic drawing of the LFT (color online)

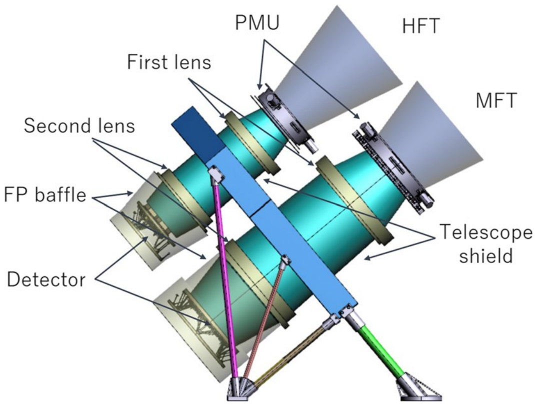

Fig. 2 Schematic drawing of the MHFT (color online)

2 Instrument Models

2.1 Telescopes

The payload module of *LiteBIRD* consists of three telescopes: the low-frequency (LFT) [6], mid-frequency (MFT), and high-frequency telescopes (HFT) [7]. For this work, we considered the MFT and HFT as an integrated telescope system, called MHFT. Schematics of the LFT and MHFT are shown in Figs. 1 and 2, respectively. Table 1 summarizes the telescope optical components and their respective temperatures. A polarization modulation unit (PMU) [8, 9] is placed in front of the aperture of each telescope to modulate a polarized CMB signal by rotating a half-wave plate (HWP) [10, 11] using a rotating mechanism with superconducting magnets. The telescopes are shielded by shields with millimeter-wave absorbers. Focal plane (FP) baffles are placed in front of the FPs.

Table 1 Telescope optical components and their assumed temperatures

LFT		MHFT	
Component	*T* (K)	Component	*T* (K)
PMU	20.0	PMU	20.0
Telescope shield	5.0	Telescope shield	5.0
Primary mirror	5.0	First lens	5.0
Secondary mirror	5.0	Second lens	5.0
FP baffle	2.0	FP baffle	2.0
Thermal filter	2.0	Thermal filter	2.0
Detector	0.1	Detector	0.1

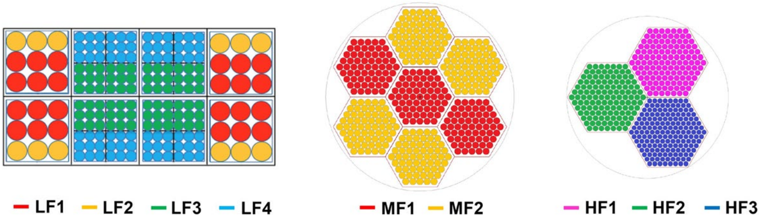

Fig. 3 Layout of the FP detector arrays of the LFT (*Left*), MFT (*Center*), and HFT (*Right*) (color online)

2.2 Focal Plane Detectors

The telescope focal planes are populated with transition-edge sensor (TES) bolometer arrays. The LFT and MFT detector arrays consist of dichroic and trichroic detectors with a combination of sinuous antennas and silicon lenslets [12]. The HFT detector array consists of monochromatic and dichroic detectors with orthomode transducers and silicon feedhorns [13]. The FP layouts are shown in Fig. 3. The design parameters of the detectors, relevant for the sensitivity calculations, are summarized in Tables 2 and 3.

3 Detector Noise

3.1 Photon Noise

We estimated the photon noise of each detector by calculating the optical loading due to the thermal emission of the CMB and the telescope optical components. Each optical component's emissivity, transmittance, and reflectance were considered while calculating the optical loading. We included the contributions of the noise due to the spilled beam energy absorbed by the FP baffle, telescope shield, and PMU.

For the LFT, we calculated the fraction of beam energy absorbed by each component using a physical optics simulation [14], based on TICRA GRASP. We

Table 2 Configuration of the LFT FP detector array, where f_c is the central frequency of the band

Module	f_c (GHz)	Fractional bandwidth	Pixel size (mm)	Number of pixels	Number of detectors
LF1	40	0.30	32.0	24	48
	60	0.23	32.0	24	48
	78	0.23	32.0	24	48
LF2	50	0.30	32.0	12	24
	68	0.23	32.0	12	24
	89	0.23	32.0	12	24
LF3	68	0.23	16.0	72	144
	89	0.23	16.0	72	144
	119	0.30	16.0	72	144
LF4	78	0.23	16.0	72	144
	100	0.23	16.0	72	144
	140	0.30	16.0	72	144
Total					1080

Table 3 Configuration of the MHFT FP detector arrays

Module	f_c (GHz)	Fractional bandwidth	Pixel size (mm)	Number of pixels	Number of detectors
MF1	100	0.23	12.0	183	366
	140	0.30	12.0	183	366
	195	0.30	12.0	183	366
MF2	119	0.30	12.0	244	488
	166	0.30	12.0	244	488
HF1	195	0.30	7.0	127	254
	280	0.30	7.0	127	254
HF2	235	0.30	7.0	127	254
	337	0.30	7.0	127	254
HF3	402	0.23	6.1	169	338
Total					3428

estimated the beam shape of the LFT detector pixel used as a feed pattern in the GRASP simulation using ANSYS HFSS.

Noise contributions due to reflections and scatterings at the optical surfaces were considered in the calculations. We assumed that finite beam energy emitted from the FP reflects on the HWP and scatters on the mirrors are absorbed by 5-K absorbers on the telescope shield. The 0.17-K TES bolometers absorb reflections from the thermal filter and detector module.

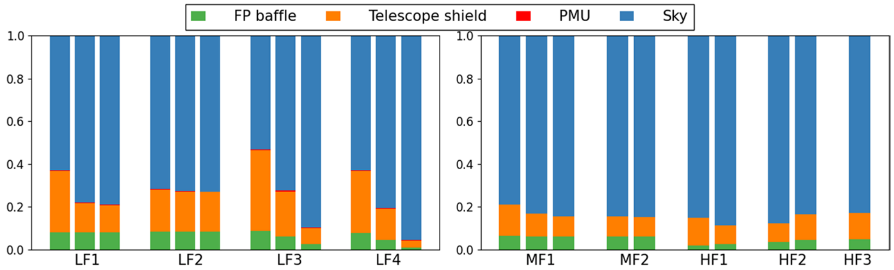

Fig. 4 Fractions of beam energy absorbed at different temperatures (2K FP baffle, 5K telescope shield, 20K PMU, and 2.7K sky) for the LFT (*left*) and MHFT (*right*). The order of the bars in each module group corresponds to that of the bands in the detector module. The contributions of the reflections are not included. (color online)

In the case of MHFT, we performed a ray-tracing analysis using Beam 4 [15] to calculate the fractions of the beam energy going to the sky and absorbed by the telescope shield and FP baffle. In addition, second-order reflections were included in the noise calculations. We included the beam patterns of the feed horns in the calculation by assuming designed beam sizes and sidelobe levels.

The fractions of beam energy absorbed at different temperatures are shown in Fig. 4.

For a given frequency band, we used the following equation to calculate the photon noise equivalent power (NEP): [5]

$$\mathrm{NEP}_{\mathrm{ph}}^2 = \int_{\nu_1}^{\nu_2} \left(2h\nu \sum_i^{N_{\mathrm{elem}}} P_i(\nu) + 2\left(\sum_i^{N_{\mathrm{elem}}} P_i(\nu) \right)^2 \right) \mathrm{d}\nu, \tag{1}$$

where ν_1 and ν_2 are the lowest and highest frequencies of the band, respectively, P_i is the optical power of element i, and N_{elem} is the number of elements in the telescope. The frequency-dependent optical efficiency from the telescope aperture to the detector was considered when calculating P_i.[1] We assumed a unitary bandpass and are planning to implement realistic bandpass shapes in the near future.

3.2 Thermal Carrier Noise

The NEP associated with the thermal carrier noise NEP_g was included in the detector noise calculation and estimated using the following equation [16]

$$\mathrm{NEP}_g = \sqrt{4k_B P_{\mathrm{oper}} T_b \frac{(n+1)^2}{2n+3} \frac{(T_c/T_b)^{2n+3} - 1}{\left[(T_c/T_b)^{n+1} - 1\right]^2}}, \tag{2}$$

[1] The detailed description for the optical power calculation can be found in Eqs. (1)–(3) of [5].

where T_c is the critical temperature, T_b is the bath temperature, P_{oper} is the operating power of the bolometer, and n is the thermal carrier index. We assumed $T_b = 0.100$ K, $T_c = 0.171$ K, and $n = 3$ because the thermal carrier is a phonon. P_{oper} is given by $P_{\mathrm{oper}} = 2.5\,P_{\mathrm{opt}}$, where P_{opt} is the optical power. The factor of 2.5 is taken over from the detector design of the *POLARBEAR2* experiment [17]. The factor optimization for *LiteBIRD* will be studied in the near future.

3.3 Readout Noise

We estimated the readout NEP due to the current noise from superconducting quantum interference device (SQUID) readout as follows:

$$\mathrm{NEP}_{\mathrm{read}} = \sqrt{P_{\mathrm{oper}}\frac{R}{2}} \times \mathrm{NEI}, \tag{3}$$

where NEI is the readout noise-equivalent current, and R is the operating resistance. We assumed $\mathrm{NEI} = 5\ \mathrm{pA}/\sqrt{\mathrm{Hz}}$ and $R = 0.8\ \Omega$ [18].[2]

3.4 Total Detector Noise

We defined the total NEP of a single detector $\mathrm{NEP}_{\mathrm{det}}$ as

$$\mathrm{NEP}_{\mathrm{det}} = \sqrt{\mathrm{NEP}_{\mathrm{ph}}^2 + \mathrm{NEP}_g^2 + \mathrm{NEP}_{\mathrm{read}}^2 + \mathrm{NEP}_{\mathrm{ext}}^2}, \tag{4}$$

where $\mathrm{NEP}_{\mathrm{ext}}$ denotes the external noise (or environment) including electromagnetic interference, microphonics, and temperature fluctuation. All the components are assumed to be mutually uncorrelated. We require that $\mathrm{NEP}_{\mathrm{ext}}$ increases $\mathrm{NEP}_{\mathrm{det}}$ by less than 15%.

4 Polarization Sensitivity

We calculated the noise equivalent temperature (NET) of a detector as [19]

$$\mathrm{NET}_{\mathrm{det}} = \frac{\mathrm{NEP}_{\mathrm{det}}}{\sqrt{2}\,(\mathrm{d}P/\mathrm{d}T_{\mathrm{CMB}})} \tag{5}$$

[2] We plan to put a SQUID readout system on the 0.1 K temperature stage to minimize the value of NEI. [18] reported the SQUIDs noise of 3.5–3.7 $\mathrm{pA}/\sqrt{\mathrm{Hz}}$ in the room temperature system.

where we have defined the conversion factor from power to CMB temperature units as [19]

$$\mathrm{d}P/\mathrm{d}T_{\mathrm{CMB}} = \int_{\nu_1}^{\nu_2} \left[\frac{\eta(\nu)}{k_B} \left(\frac{h\nu}{T_{\mathrm{CMB}}(e^{h\nu/k_B T_{\mathrm{CMB}}} - 1)} \right)^2 e^{h\nu/k_B T_{\mathrm{CMB}}} \right] \mathrm{d}\nu \tag{6}$$

where ν_1 and ν_2 are the edges of the band. η is end-to-end optical efficiency including the transmittances of the PMU, mirrors, lenses, thermal filter, the aperture and detector efficiencies, and the polarization efficiency of the PMU. The array NET was obtained as follows:

$$\mathrm{NET}_{\mathrm{arr}} = \frac{\mathrm{NET}_{\mathrm{det}}}{\sqrt{0.8 \times N_{\mathrm{det}}}}, \tag{7}$$

where $\mathrm{NET}_{\mathrm{det}}$ is the NET of the single detector, N_{det} is the number of detectors, and the factor of 0.8 corresponds to the degradation of the detector yield.[3]

The polarization sensitivity in unit of $\mu\mathrm{K} \cdot \mathrm{arcmin}$ was calculated as

$$\sigma_S = \sqrt{\frac{4\pi f_{\mathrm{sky}}\, 2\, \mathrm{NET}_{\mathrm{arr}}{}^2}{t_{\mathrm{obs}}}} \left(\frac{10800}{\pi} \right), \tag{8}$$

where f_{sky} is the sky coverage fraction, and t_{obs} is the observation time. Here, $f_{\mathrm{sky}} = 1.0$ and $t_{\mathrm{obs}} = 3$ years (94,672,800 s) $\times$ 0.767, considering the observation duty cycle of 85%,[4] cosmic-ray hits (5%), and marginal loss (5%). The $\sqrt{2}$ factor that accompanies $\mathrm{NET}_{\mathrm{arr}}$ accounts for the need for two detectors to measure the CMB polarization. The noise components of the detector bands and the sensitivities of the observation bands are listed in Tables 4 and 5, respectively.

5 Conclusions

Sensitivity estimations have been presented using the current *LiteBIRD* experimental design. To accurately estimate the detector noise originating from the optical loading, we introduced optical simulations based on physical optics and ray tracing for the LFT and MHFT, respectively. Preliminary forecasts in the presence of instrumental systematics and astrophysical foregrounds show that the current *LiteBIRD* configuration satisfies the requirements of $\delta r \leq 1.0 \times 10^{-3}$ [3]. As the instrumental modeling and experimental design evolve, we expect to refine and update the provided sensitivity estimates.

[3] The *SPT-3G* experiment reported the integrated performance in [20]. They report an operable detector yield of 90 % approximately. We assumed the detector yield of 80 % as a conservative value.

[4] The observation duty cycle includes the recycling of an adiabatic demagnetization refrigerator, data transfer, and detector tuning.

Table 4 Noise components for each detector band and for each telescope

Telescope	f_c (GHz)	NEP_{ph}	NEP_g	NEP_{read}	NEP_{ext}	NEP_{det}	NET_{det}	NET_{arr}
LFT	40	5.44	3.95	2.67	4.09	8.31	114.63	18.50
	60	5.26	3.59	2.43	3.86	7.84	65.28	10.54
	78	5.98	3.79	2.57	4.26	8.65	58.61	9.46
	50	5.72	4.04	2.74	4.25	8.64	72.48	16.54
	68	5.81	3.80	2.58	4.19	8.51	68.81	15.70
	89	6.58	3.97	2.69	4.61	9.36	62.33	14.22
	68	6.58	4.18	2.83	4.69	9.53	105.64	9.84
	89	6.85	4.11	2.78	4.79	9.72	65.18	6.07
	119	8.18	4.48	3.04	5.55	11.27	40.78	3.80
	78	6.76	4.18	2.83	4.77	9.69	82.51	7.69
	100	6.97	4.04	2.74	4.81	9.78	54.88	5.11
	140	8.45	4.36	2.95	5.63	11.44	38.44	3.58
MFT	100	7.62	4.36	2.95	5.24	10.64	71.70	4.19
	119	8.92	4.84	3.28	6.03	12.25	55.65	2.82
	140	9.27	4.74	3.21	6.16	12.52	54.00	3.16
	166	9.56	4.57	3.09	6.24	12.68	54.37	2.75
	195	9.78	4.37	2.96	6.29	12.77	59.61	3.48
HFT	195	13.23	5.79	3.93	8.46	17.19	73.96	5.19
	235	12.31	5.01	3.40	7.76	15.77	76.06	5.34
	280	11.91	4.49	3.04	7.40	15.04	97.26	6.82
	337	11.58	4.00	2.71	7.10	14.42	154.64	10.85
	402	10.85	3.43	2.32	6.57	13.34	385.69	23.45

The units of NEP and NET are $aW/\sqrt{Hz}$ and $\mu K\sqrt{sec}$, respectively . The factor of $\sqrt{2}$ has not yet been included in the NET_{arr} column

Table 5 Polarization sensitivity values for each of the LiteBIRD observation bands

f_c (GHz)	Sensitivity (μK $\cdot$ arcmin)
40	37.42
50	33.46
60	21.31
68	16.87
78	12.07
89	11.30
100	6.56
119	4.58
140	4.79
166	5.57
195	5.85
235	10.79
280	13.80
337	21.95
402	47.45
Overall sensitivity	2.16

Overall sensitivity is given by the inverse-variance weighted sum of the band sensitivities

Acknowledgements This work is supported in Japan by ISAS/JAXA for Pre-Phase A2 studies, by the acceleration program of JAXA research and development directorate, by the World Premier International Research Center Initiative (WPI) of MEXT, by the JSPS Core-to-Core Program of A. Advanced Research Networks, and by JSPS KAKENHI Grant Numbers JP15H05891, JP17H01115, and JP17H01125. The Italian LiteBIRD phase A contribution is supported by the Italian Space Agency (ASI Grants No. 2020-9-HH.0 and 2016-24-H.1-2018), the National Institute for Nuclear Physics (INFN), the National Institute for Astrophysics (INAF), and the Italian Ministry of Foreign Affairs and International Cooperation. The French LiteBIRD phase A contribution is supported by the Centre National d'Etudes Spatiale (CNES), by the Centre National de la Recherche Scientifique (CNRS), and by the Commissariat à l'Energie Atomique (CEA). The Canadian contribution is supported by the Canadian Space Agency. The US contribution is supported by NASA grant no. 80NSSC18K0132. Norwegian participation in LiteBIRD is supported by the Research Council of Norway (Grant No. 263011). The Spanish LiteBIRD phase A contribution is supported by the Spanish Agencia Estatal de Investigación (AEI), project refs. PID2019-110610RB-C21 and AYA2017-84185-P. Funds that support the Swedish contributions come from the Swedish National Space Agency (SNSA/Rymdstyrelsen) and the Swedish Research Council (Reg. no. 2019-03959). The German participation in LiteBIRD is supported in part by the Excellence Cluster ORIGINS, which is funded by the Deutsche Forschungsgemeinschaft (DFG, German Research Foundation) under Germany's Excellence Strategy (Grant No. EXC-2094 - 390783311). This research used resources of the Central Computing System owned and operated by the Computing Research Center at KEK, as well as resources of the National Energy Research Scientific Computing Center, a DOE Office of Science User Facility supported by the Office of Science of the U.S. Department of Energy.

References

1. M. Hazumi et al., Proc. SPIE **114432F** (2020)
2. A.A. Starobinsky, Pisma. Zh. Eksp. Teor. Fiz **30**, 719 (1979)
3. E. Allys et al., arXiv:2202.02773v1 (2022)
4. T. Hasebe et al., J. Low Temp. Phys. **193**(5), 841 (2018)

5. C.A. Hill et al., Proc. SPIE **1070842** (2018)
6. Y. Sekimoto et al., Proc. SPIE **1145310** (2020)
7. L. Montier et al., Proc. SPIE **114432G** (2020)
8. Y. Sakurai et al., Proc. SPIE **114534E** (2020)
9. F. Columbro et al., Proc. SPIE **114436Z** (2020)
10. K. Komatsu et al., J. Astron. Telesc. Instrum. Syst. **7**(3), 034005 (2021)
11. G. Pisano et al., Progress in Electromagnetics Research M **25**, 101 (2012)
12. B. Westbrook et al., Proc. SPIE **114435Q** (2020)
13. S. Walker et al., J. Low. Temp. Phys. **199**, 891 (2020)
14. H. Imada et al., Proc. SPIE **10698** (2018)
15. Stellarsoftware website, https://www.stellarsoftware.com
16. A. Suzuki, *Ph.D. dissertation* University of California, Berkeley (2013)
17. Z.D. Kermish et al., Proc. SPIE **84521C** (2012)
18. M.A. Dobbs et al., Rev. Sci. Instrum. **83**(073113) (2012)
19. K. Arnold, *Ph.D. dissertation* University of California, Berkeley (2010)
20. J.A. Sobrin et al., Astrophys. J. **258**(42) (2022)

Authors and Affiliations

T. Hasebe[1] · P. A. R. Ade[2] · A. Adler[3] · E. Allys[4] · D. Alonso[5] · K. Arnold[6] · D. Auguste[7] · J. Aumont[8] · R. Aurlien[9] · J. Austermann[10] · S. Azzoni[1,5] · C. Baccigalupi[11,12,13] · A. J. Banday[8] · R. Banerji[9] · R. B. Barreiro[14] · N. Bartolo[15,16] · S. Basak[17] · E. Battistelli[18,19] · L. Bautista[8] · J. Beall[10] · D. Beck[20] · S. Beckman[21] · K. Benabed[22] · J. Bermejo-Ballesteros[23] · M. Bersanelli[24,25] · J. Bonis[7] · J. Borrill[26] · F. Bouchet[22] · F. Boulanger[4] · S. Bounissou[27] · M. Brilenkov[9] · M. L. Brown[28] · M. Bucher[29] · E. Calabrese[2] · M. Calvo[30] · P. Campeti[31] · A. Carones[32,33] · F. J. Casas[14] · A. Catalano[34] · A. Challinor[35,36,37] · V. Chan[38] · K. Cheung[21,26,39] · Y. Chinone[1,40] · J. Cliche[41] · F. Columbro[18,19] · W. Coulton[1] · J. Cubas[23] · A. Cukierman[20,21] · D. Curtis[39] · G. D'Alessandro[18,19] · K. Dachlythra[3] · P. de Bernardis[18,19] · T. de Haan[42] · E. de la Hoz[14,43] · M. De Petris[18,19] · S. Della Torre[44] · C. Dickinson[28] · P. Diego-Palazuelos[14,43] · M. Dobbs[41] · T. Dotani[45,46] · D. Douillet[7] · L. Duband[47] · A. Ducout[1] · S. Duff[10] · J. M. Duval[47] · K. Ebisawa[45] · T. Elleflot[26] · H. K. Eriksen[9] · J. Errard[29] · T. Essinger-Hileman[48] · F. Finelli[49,50] · R. Flauger[6] · C. Franceschet[24,25] · U. Fuskeland[9] · S. Galli[22] · M. Galloway[9] · K. Ganga[29] · J. R. Gao[51] · R. T. Genova-Santos[52,53] · M. Gerbino[54] · M. Gervasi[44,55] · T. Ghigna[1,5] · S. Giardiello[56] · E. Gjerløw[9] · M. L. Gradziel[57] · J. Grain[27] · L. Grandsire[29] · F. Grupp[58] · A. Gruppuso[49,50] · J. E. Gudmundsson[3] · N. W. Halverson[59] · J. Hamilton[29] · P. Hargrave[2] · M. Hasegawa[42] · M. Hattori[60] · M. Hazumi[1,42,45,46] · S. Henrot-Versillé[7] · L. T. Hergt[61] · D. Herman[9] · D. Herranz[14] · C. A. Hill[21,62] · G. Hilton[10] · E. Hivon[22] · R. A. Hlozek[38] · T. D. Hoang[63] · A. L. Hornsby[21] · Y. Hoshino[64] · J. Hubmayr[10] · K. Ichiki[65] · T. Iida[66] · H. Imada[67] · K. Ishimura[68] · H. Ishino[69] · G. Jaehnig[59] · M. Jones[5] · T. Kaga[70] · S. Kashima[67] ·

N. Katayama[1] · A. Kato[42] · T. Kawasaki[71] · R. Keskitalo[21,26,39] · T. Kisner[26] · Y. Kobayashi[72,73] · N. Kogiso[74] · A. Kogut[48] · K. Kohri[42] · E. Komatsu[31] · K. Komatsu[69] · K. Konishi[75] · N. Krachmalnicoff[11,12,13] · I. Kreykenbohm[76] · C. L. Kuo[20,77] · A. Kushino[78] · L. Lamagna[18,19] · J. V. Lanen[10] · G. Laquaniello[7] · M. Lattanzi[54] · A. T. Lee[21,62] · C. Leloup[29] · F. Levrier[4] · E. Linder[39,62] · T. Louis[7] · G. Luzzi[79] · J. Macias-Perez[34] · T. Maciaszek[80] · B. Maffei[27] · D. Maino[24] · M. Maki[42] · S. Mandelli[24,25] · M. Maris[81] · E. Martínez-González[14] · S. Masi[18,19] · M. Massa[82] · S. Matarrese[15,16,83,84] · F. T. Matsuda[45] · T. Matsumura[1] · L. Mele[18,19] · A. Mennella[24,25] · M. Migliaccio[32,33] · Y. Minami[85] · K. Mitsuda[67] · A. Moggi[82] · A. Monfardini[30] · J. Montgomery[41] · L. Montier[8] · G. Morgante[49] · B. Mot[8] · Y. Murata[45] · J. A. Murphy[86] · M. Nagai[67] · Y. Nagano[69] · T. Nagasaki[42] · R. Nagata[45] · S. Nakamura[87] · R. Nakano[45,73] · T. Namikawa[35,37] · F. Nati[44,55] · P. Natoli[54,56] · S. Nerval[38] · T. Nishibori[70] · H. Nishino[42] · F. Noviello[2] · C. O'Sullivan[57] · K. Odagiri[45] · H. Ogawa[74] · H. Ogawa[45] · S. Oguri[45] · H. Ohsaki[72] · I. S. Ohta[88] · N. Okada[70] · N. Okada[74] · L. Pagano[27,54,56] · A. Paiella[18,19] · D. Paoletti[49,50] · A. Passerini[44,55] · G. Patanchon[29] · V. Pelgrim[89] · J. Peloton[7] · F. Piacentini[18,19] · M. Piat[29] · G. Pisano[18] · G. Polenta[79] · D. Poletti[44,55] · T. Prouvé[47] · G. Puglisi[39] · D. Rambaud[8] · C. Raum[21] · S. Realini[24] · M. Reinecke[31] · M. Remazeilles[28] · A. Ritacco[4,27] · G. Roudil[8] · J. Rubino-Martin[52,53] · M. Russell[6] · H. Sakurai[72] · Y. Sakurai[1,69] · M. Sandri[49] · M. Sasaki[76] · G. Savini[90] · D. Scott[61] · J. Seibert[6] · Y. Sekimoto[42,45,73] · B. Sherwin[35,37,62] · K. Shinozaki[70] · M. Shiraishi[91] · P. Shirron[48] · G. Signorelli[82] · G. Smecher[41,92] · F. Spinella[82] · S. Stever[1,69] · R. Stompor[29,93] · S. Sugiyama[64] · R. Sullivan[61] · A. Suzuki[26] · J. Suzuki[42] · T. L. Svalheim[9] · E. Switzer[48] · R. Takaku[45,94] · H. Takakura[45,73] · S. Takakura[1] · Y. Takase[69] · Y. Takeda[70] · A. Tartari[82,95] · D. Tavagnacco[49] · A. Taylor[5] · E. Taylor[21] · Y. Terao[72] · J. Thermeau[29] · H. Thommesen[9] · K. L. Thompson[20,77] · B. Thorne[5] · T. Toda[69] · M. Tomasi[24,25] · M. Tominaga[45,94] · N. Trappe[57] · M. Tristram[7] · M. Tsuji[91] · M. Tsujimoto[45] · C. Tucker[2] · J. Ullom[10] · L. Vacher[8] · G. Vermeulen[30] · P. Vielva[14] · F. Villa[49] · M. Vissers[10] · N. Vittorio[32,33] · B. Wandelt[22] · W. Wang[29] · K. Watanuki[45] · I. K. Wehus[9] · J. Weller[58] · B. Westbrook[21] · J. Wilms[76] · B. Winter[90,96] · E. J. Wollack[48] · N. Y. Yamasaki[45] · T. Yoshida[45] · J. Yumoto[72] · A. Zacchei[81] · M. Zannoni[44,55] · A. Zonca[97] · LiteBIRD Collaboration

✉ T. Hasebe
takashihasebe.u@gmail.com

1 Kavli Institute for the Physics and Mathematics of the Universe (Kavli IPMU, WPI), UTIAS, The University of Tokyo, Kashiwa, Chiba 277-8583, Japan

2 School of Physics and Astronomy, Cardiff University, Cardiff CF10 3XQ, UK

3 Department of Physics, The Oskar Klein Centre, Stockholm University, 106 91 Stockholm, Sweden

4 Laboratoire de Physique de l' École Normale Sup´erieure, ENS, Université PSL, CNRS, Sorbonne Université, Université de Paris, 75005 Paris, France

5 Department of Physics, University of Oxford, Denys Wilkinson Building, Keble Road, Oxford OX1 3RH, UK

[6] Department of Physics, University of California, San Diego, San Diego, CA 92093-0424, USA

[7] CNRS/IN2P3, IJCLab, Université Paris-Saclay, 91405 Orsay, France

[8] IRAP, Université de Toulouse, CNRS, CNES, UPS, Toulouse, France

[9] Institute of Theoretical Astrophysics, University of Oslo, Blindern, Oslo, Norway

[10] National Institute of Standards and Technology (NIST), Boulder, CO 80305, USA

[11] International School for Advanced Studies (SISSA), Via Bonomea 265, 34136 Trieste, Italy

[12] INFN Sezione di Trieste, Via Valerio 2, 34127 Trieste, Italy

[13] IFPU, Via Beirut, 2, 34151 Grignano, Trieste, Italy

[14] Instituto de Fisica de Cantabria (IFCA, CSIC-UC), Avenida los Castros SN, 39005 Santander, Spain

[15] Dipartimento di Fisica e Astronomia "G. Galilei", Universita ' degli Studi di Padova, Via Marzolo 8, 35131 Padova, Italy

[16] INFN Sezione di Padova, Via Marzolo 8, 35131 Padova, Italy

[17] School of Physics, Indian Institute of Science Education and Research Thiruvananthapuram, Maruthamala PO, Vithura, Thiruvananthapuram, Kerala 695551, India

[18] Dipartimento di Fisica, Università La Sapienza, P. le A. Moro 2, Rome, Italy

[19] INFN Sezione di Roma, P.le A. Moro 2, 00185 Rome, Italy

[20] Department of Physics, Stanford University, Stanford, CA 94305-4060, USA

[21] Department of Physics, University of California, Berkeley, Berkeley, CA 94720, USA

[22] Institut d'Astrophysique de Paris, CNRS/Sorbonne Université, Paris, France

[23] Instituto Universitario "Ignacio Da Riva" (IDR/UPM), Universidad Politécnica de Madrid, Plaza Cardenal Cisneros, 3, 28040 Madrid, Spain

[24] Dipartimento di Fisica, Universita' degli Studi di Milano, Via Celoria 16, 20133 Milan, Italy

[25] INFN Sezione di Milano, Via Celoria 16, 20133 Milan, Italy

[26] Computational Cosmology Center, Lawrence Berkeley National Laboratory (LBNL), Berkeley, CA 94720, USA

[27] CNRS, Institut d'Astrophysique Spatiale, Université Paris-Saclay, 91405 Orsay, France

[28] University of Manchester, Manchester M13 9PL, UK

[29] AstroParticle and Cosmology (APC) - University Paris Diderot, CNRS/IN2P3, CEA/Irfu, Obs de Paris, Sorbonne Paris Cité, Paris, France

[30] CNRS, Grenoble INP, Institut Néel, Univ. Grenoble Alpes, 38000 Grenoble, France

[31] Max-Planck-Institute for Astrophysics, Garching, Germany

[32] Dipartimento di Fisica, Università di Roma Tor Vergata, Via della Ricerca Scientifica, 1, 00133 Rome, Italy

[33] INFN Sezione di Roma2, Università di Roma Tor Vergata, Via della Ricerca Scientifica, 1, 00133 Rome, Italy

[34] CNRS, LPSC-IN2P3, Univ. Grenoble Alpes, 53, Avenue des Martyrs, 38000 Grenoble, France

[35] DAMTP, Centre for Mathematical Sciences, Wilberforce Road, Cambridge CB3 0WA, UK

[36] Institute of Astronomy, Madingley Road, Cambridge CB3 0HA, UK

[37] Kavli Institute for Cosmology Cambridge, Madingley Road, Cambridge CB3 0HA, Canada

[38] David A. Dunlap Department of Astronomy and Astrophysics, 50 St. George Street, Toronto,

ON M5S3H4, Canada

[39] Space Science Laboratory, University of California, Berkeley, Berkeley, CA 94720, USA

[40] School of Science, Research Center for the Early Universe, RESCEU, University of Tokyo, Tokyo, Japan

[41] Physics Department, McGill University, Montreal, QC H3A 0G4, Canada

[42] High Energy Accelerator Research Organization (KEK), Tsukuba, Ibaraki 305-0801, Japan

[43] Dpto. de Física Moderna, Universidad de Cantabria, Avda. los Castros s/n, 39005 Santander, Spain

[44] INFN Sezione Milano Bicocca, Piazza della Scienza, 3, 20126 Milan, Italy

[45] Institute of Space and Astronautical Science (ISAS), Japan Aerospace Exploration Agency (JAXA), Sagamihara, Kanagawa 252-5210, Japan

[46] The Graduate University for Advanced Studies (SOKENDAI), Miura District, Hayama, Kanagawa 240-0115, Japan

[47] CEA, IRIG-DSBT, Université Grenoble Alpes, 38000 Grenoble, France

[48] NASA Goddard Space Flight Center, Greenbelt, MD, USA

[49] INAF - OAS Bologna, Via Piero Gobetti, 93/3, 40129 Bologna, Italy

[50] INFN Sezione di Bologna, Viale C. Berti Pichat, 6/2, 40127 Bologna, Italy

[51] SRON Netherlands Institute for Space Research, Sorbonnelaan 2, 3584 CA Utrecht, The Netherlands

[52] Instituto de Astrofísica de Canarias, 38200 La Laguna, Tenerife, Canary Islands, Spain

[53] Departamento de Astrofísica, Universidad de La Laguna (ULL), 38206 La Laguna, Tenerife, Spain

[54] INFN Sezione di Ferrara, Via Saragat 1, 44122 Ferrara, Italy

[55] Physics Department, University of Milano Bicocca, p.zza della Scienza, 3, 20126 Milan, Italy

[56] Dipartimento di Fisica e Scienze della Terra, Università di Ferrara, Via Saragat 1, 44122 Ferrara, Italy

[57] National University of Ireland Maynooth, Maynooth, Ireland

[58] USM, The Ludwig Maximilians University of Munich, Munich, Germany

[59] Center for Astrophysics and Space Astronomy, University of Colorado, Boulder, CO 80309, USA

[60] Graduate School of Science, Astronomical Institute, Tohoku University, Sendai 980-8578, Japan

[61] Department of Physics and Astronomy, University of British Columbia, 6224 Agricultural Road, Vancouver, BC V6T1Z1, Canada

[62] Physics Division, Lawrence Berkeley National Laboratory (LBNL), Berkeley, CA 94720, USA

[63] University of Science and Technology of Hanoi, Hanoi, Vietnam

[64] Saitama University, Saitama 338-8570, Japan

[65] Kobayashi-Masukawa Institute for the Origin of Particle and the Universe, Nagoya University, Aichi 464-8602, Japan

[66] ispace, inc., Tokyo, Japan

[67] National Astronomical Observatory of Japan, Mitaka, Tokyo 181-8588, Japan

[68] Waseda University, Tokyo, Japan

[69] Department of Physics, Okayama University, Okayama 700-8530, Japan

[70] Research and Development Directorate, Japan Aerospace Exploration Agency (JAXA), Tsukuba, Ibaraki 305-8505, Japan

[71] Kitasato University, Sagamihara, Kanagawa 252-0373, Japan

[72] The Institute for Solid State Physics (ISSP), The University of Tokyo, Kashiwa, Chiba 277-8581, Japan

[73] Department of Astronomy, The University of Tokyo, Tokyo 113-0033, Japan

[74] Osaka Prefecture University, Sakai, Osaka 599-8531, Japan

[75] Institute for Photon Science and Technology, The University of Tokyo, Tokyo, Japan

[76] Remeis-Observatory and Erlangen Centre for Astroparticle Physics, FAU Erlangen-Nürnberg, Sternwartstr. 7, 96049 Bamberg, Germany

[77] SLAC National Accelerator Laboratory, Kavli Institute for Particle Astrophysics and Cosmology (KIPAC), Menlo Park, CA 94025, USA

[78] Kurume University, Kurume, Fukuoka 830-0011, Japan

[79] Space Science Data Center, Italian Space Agency, Via del Politecnico, 00133 Rome, Italy

[80] Centre National d'Etudes Spatiales (CNES), Paris, France

[81] INAF - Astronomical Observatory of Trieste, Trieste, Italy

[82] INFN Sezione di Pisa, Largo Bruno Pontecorvo 3, 56127 Pisa, Italy

[83] INAF, Osservatorio Astronomico di Padova, Vicolo dell'Osservatorio 5, 35122 Padova, Italy

[84] Gran Sasso Science Institute (GSSI), Viale F. Crispi 7, 67100 L'Aquila, Italy

[85] Research Center for Nuclear Physics, Osaka University, Osaka, Ibaraki 567-0047, Japan

[86] National University of Ireland Maynooth, Maynooth, Ireland

[87] Yokohama National University, Yokohama, Kanagawa 240-8501, Japan

[88] Konan University, Kobe, Japan

[89] Institute of Astrophysics, FORTH, Heraklion, Greece

[90] Physics and Astronomy Department, University College London (UCL), London, UK

[91] National Institute of Technology, Kagawa College, Mitoyo, Japan

[92] Three-Speed Logic, Inc., Victoria, Canada

[93] CNRS-UCB International Research Laboratory, Centre Pierre Binétruy, UMI2007, Berkeley, CA 94720, USA

[94] Department of Physics, The University of Tokyo, Tokyo 113-0033, Japan

[95] Dipartimento di Fisica, Università di Pisa, Largo B. Pontecorvo 3, 56127 Pisa, Italy

[96] Mullard Space Science Laboratory, University College London, London, UK

[97] San Diego Supercomputer Center, University of California, San Diego, La Jolla, CA, USA